

See discussions, stats, and author profiles for this publication at: <https://www.researchgate.net/publication/281786164>

Direction Controlled Methane Hydrate Growth

ARTICLE *in* CRYSTAL GROWTH & DESIGN · SEPTEMBER 2015

Impact Factor: 4.89 · DOI: 10.1021/acs.cgd.5b01070

CITATION

1

READS

19

7 AUTHORS, INCLUDING:



Fei Wang

Chinese Academy of Sciences

13 PUBLICATIONS 21 CITATIONS

SEE PROFILE

Direction Controlled Methane Hydrate Growth

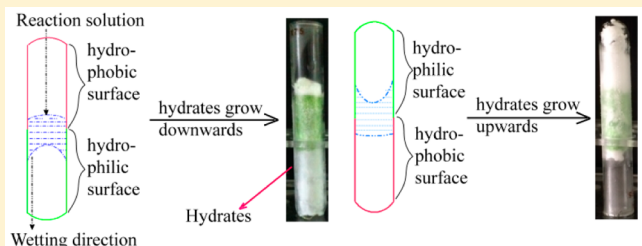
Fei Wang,^{†,‡} Lin Wang,[†] Chuanshui Wang,[†] Gang Guo,[†] Guoqiang Liu,[§] Shengjun Luo,^{*,†} and Rongbo Guo^{*,†}

[†]Shandong Industrial Engineering Laboratory of Biogas Production and Utilization, Key Laboratory of Biofuels, Qingdao Institute of Bioenergy and Bioprocess Technology, Chinese Academy of Sciences, Qingdao 266101, Shandong China

[‡]University of Chinese Academy of Science, Beijing 10049, China

[§]Qingdao University of Science & Technology, Qingdao 266042, China

ABSTRACT: Gas hydrate growth pattern is of great importance in hydrate-based gas storage and transportation. In this work, direction controlled methane hydrate growth in the presence of sodium dodecyl sulfate (SDS) was achieved through hydrophobic modification to the hydrate growth surface and design to the existing manner of the reaction solution in the reactor. Upward methane hydrate growth was obtained when the hydrate formation took place on hydrophilic surface, while when the hydrate growth surface was hydrophobically modified, the upward hydrate growth was retarded. Downward hydrate growth was accomplished by fixing the reaction solution in the middle part of the reactor, because both gravity and capillary effect promoted the downward hydrate growth. However, when the lower part of the reactor was hydrophobically modified, the downward hydrate growth was restrained and upward hydrate growth was achieved.



INTRODUCTION

Biogas, converted from organic waste, is considered as one of the most important renewable energy sources due to the low environmental impact and high energy conversion efficiency during production.^{1–3} Biomethane, refined from biogas, is regarded as a potential substitute of natural gas. Moreover, the production of biomethane is regionally distributed, which can exactly meet the regional dispersibility of biomethane utilization, especially for the remote areas.

Natural gas hydrates, formed by natural gas and water molecules at appropriate pressure and temperature,⁴ are of great potential in natural gas storage and transportation due to the high storage capacity and good storage security.^{5,6} Therefore, storing biomethane in hydrates with suitable vessels (e.g., m³ level) for direct utilization can achieve the energy storage and transportation with high energy density and low cost, which is of great significance for remote areas. However, several problems have to be resolved for the hydrate-based biomethane storage and transportation, such as the long induction period and low growth rate during the hydrate formation process.^{7,8}

Surfactants, such as sodium dodecyl sulfate (SDS), have been confirmed to promote the hydrate formation efficiently because surfactants could change the hydrate formation pattern.^{9–13} In the quiescent deionized water–gas system, hydrates initially formed as a thin film at the gas/liquid interface and then grew downward as dendrites into the bulk water.¹⁴ However, the existence of the hydrate film at the gas/liquid interface hindered the further diffusion of gas into the aqueous phase and therefore resulted in slow hydrate growth.⁷ While in the hydrate

formation with SDS as promoter, as reported by Gayet et al.,⁹ SDS molecules could prevent the hydrate particles from gathering to form a hydrate film at the gas/liquid interface and hydrates mainly formed on the reactor sidewall as porous structures. Afterward the reaction solution could be sucked to the hydrate surface through the porous structures under capillary force, leading to the hydrates growing upward on the reactor sidewall. As a result, no hydrate film was formed at the gas/liquid interface and rapid hydrate growth was obtained.

However, the upward hydrate growth also led to the hydrates accumulating as highly porous layers in the upper part of the reactor with low apparent density.^{10,11} In consequence, the space utilization of the reactor was poor and further separation and compaction of the hydrates was inevitable for storage and transportation.¹⁵ Therefore, controlling the hydrate growth direction to obtain hydrates with high apparent density is of great significance in achieving the direction utilization of biomethane hydrates prepared in suitable vessels.

In our previous study,¹⁶ the contact angle (wettability) of the surfactant solution on the reactor sidewall was found from the relationship with the methane hydrate growth pattern. Low contact angle was conducive to the upward hydrate growth on the reactor sidewall, while high contact angle led to the hydrates formed mainly in the reactor bottom. In addition, when SDS was fixed on the surface of polystyrene nanospheres in methane hydrate formation, hydrates no more grew upward

Received: July 26, 2015

Revised: August 25, 2015

on the reactor sidewall but mainly formed in the bottom of the reactor with much higher apparent density.¹⁵

In this work, walls with different surface properties were used for methane hydrate formation. The existing manner of the reaction solution in the reactor was designed and the hydrophilicity of the hydrate growth surface was modified to achieve the direction controlled methane hydrate growth.

EXPERIMENTAL SECTION

Materials. Sodium dodecyl sulfate (AR) was provided by Xiya Reagent Co., Ltd. Methane (99.99%) was purchased from Heli Gas Co., Ltd. (Qingdao, China). The glass and plastic tubes were purchased from Qingdao Haiqian Chemical Co., Ltd. (Qingdao, China). Methanol was purchased from Sinopharm Chemical Reagent CO., Ltd. (Shanghai, China). The amino silicone oil was provided by Bluestar Silicones (Beijing, China). The deionized water used in this work was laboratory-made, and the conductivity was $1.1 \pm 0.1 \mu\text{s}/\text{cm}$.

Critical Micelle Concentration and Solubility of Sodium Dodecyl Sulfate. The critical micelle concentration (cmc) of SDS at 298.15 K and the solubility of SDS at hydrate formation temperature (275.15 K) were determined through conductivity method. SDS solutions were placed under 298.15 or 275.15 K for 2 h, and then the conductivities were measured with a DDSJ-318 conductivity meter (Shanghai INESA Instrument Co., Ltd.). Each experiment was carried out three times, and photographs were taken for the SDS solutions under 298.15 and 275.15 K, respectively.

Contact Angle of Sodium Dodecyl Sulfate Solution on the Reactor Inner Surface. The contact angle of the surfactant solution on the reactor inner surface was measured through gypsometry, and the details were shown in our previous study.¹⁶

Methane Hydrate Formation. The methane hydrate formation apparatus is shown in Figure 1, of which the main part consisted of a

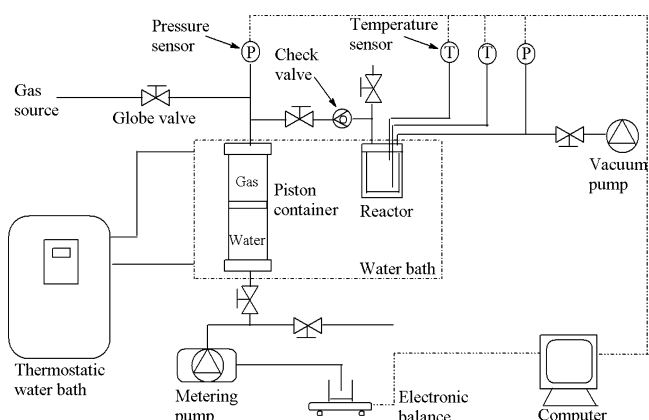


Figure 1. Schematic diagram of the hydrate formation apparatus.

piston container with the volume of 1 L and a reactor with the volume of 200 mL. In this work, methane was pressurized into the piston container in advance to reach the reaction temperature (275.15 K) and then charged into the reactor, which could avoid the pressure change in the reactor caused by the cooling process when the reactor was inflated directly.

A 50 mL aliquot of methanol solution (20 vol %) was added into the reactor, and then tubes containing 1 mL of SDS solution were placed into the methanol solution with the tube mouth above the liquid level. Given the stochasticity of hydrate formation, three tubes were used in each experiment and the schematic diagram is shown in Figure 2A. Moreover, fresh SDS solutions and new tubes were used in the each experiment. The methanol solution was used to promote the heat removal during hydrate formation and keep the three tubes in the environment with uniform heat distribution. The hydrate formation with methanol solution could be neglected as methanol was an inhibitor of hydrate formation.¹⁷ After the temperature of the reaction

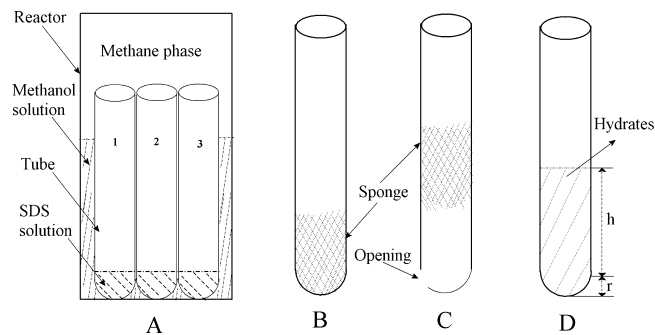


Figure 2. Schematic diagrams of the tubes in the reactor (A), the tube with a sponge fixed in the bottom (B), the tube with a sponge fixed in the middle (C), and the calculation of the cover factor (D).

solution reached 275.15 K, the reactor was vacuumed and cleaned with methane three times and then pressurized with methane to 6 MPa through the metering pump pressuring the piston container with deionized water. The temperature and pressure of the hydrate formation system were recorded on the computer during the whole process. After the completion of hydrate formation, the tubes were taken out immediately and frozen under 193.15 K to preserve the hydrate morphology in the tubes, and then photographs were taken of the tubes.

To further achieve the direction controlled hydrate growth, the existing manner of the reaction solution in the tube was designed. On one hand, the SDS solution (1 mL) was adsorbed in a sponge which was fixed in the bottom of the tube, as shown in Figure 2B. On the other hand, the sponge that contained 1 mL of SDS solution was fixed in the middle of the tube and both the top and the bottom of the tube were open, as shown in Figure 2C. It should be noted that the 50 mL of methanol solution was removed in the hydrate formation with the sponge in the middle of the tube.

Hydrophobic Modification of Glass Tubes. In the hydrophobic modification of glass tubes, the inner surface of the tube was speared with amino silicone oil and kept for 30 min, and then the speared surface was erased with lens paper repeatedly until no amino silicone oil could be observed.

Calculation of Cover Factor. To reveal the methane hydrate growth on the reactor sidewall quantitatively, a cover factor (f) was proposed in this work, which was defined as the ratio of the theoretical and practical areas of the reactor wall covered by the hydrates formed with 1 mL of SDS solution. A higher cover factor indicated the larger extent of upward hydrate growth on the reactor sidewall. The tube used in this work consisted of a cylinder and a hemisphere, as shown in Figure 2D. The cover area of hydrates consisted of the lateral area of the tubes with the hydrates height and the area of the hemisphere. Therefore, f can be calculated as follows:

$$f = \frac{\frac{4\pi r^2}{3} \times \frac{1}{2} + 2\pi r h_p}{\frac{4\pi r^2}{3} \times \frac{1}{2} + 2\pi r h_t} = \frac{1 + h_p}{1 + h_t} \quad (1)$$

where r is the inner radius of the hemisphere; h_t and h_p are the theoretical and practical heights of the hydrates on the sidewall of the tube, respectively, as shown in Figure 2D; for the glass tube, r is 0.4 cm; for the plastic tube, r is 0.6 cm.

The theoretical cover area of the hydrates was the area covered when hydrates were absolutely compact; therefore, h_t can be calculated according to the following equation:

$$\frac{4}{3}\pi r^3 \times \frac{1}{2} + 2\pi r h_t = V_h = V_w + \Delta V \frac{m_w}{M_w} \quad (2)$$

where V_h is the theoretical volume of hydrates; V_w is the volume of SDS solution; ΔV is the molar volume difference between hydrates and water, which has been reported as $4.6 \text{ cm}^3/(\text{mol of water})$; m_w is the weight of water; and M_w is the molar mass of water.

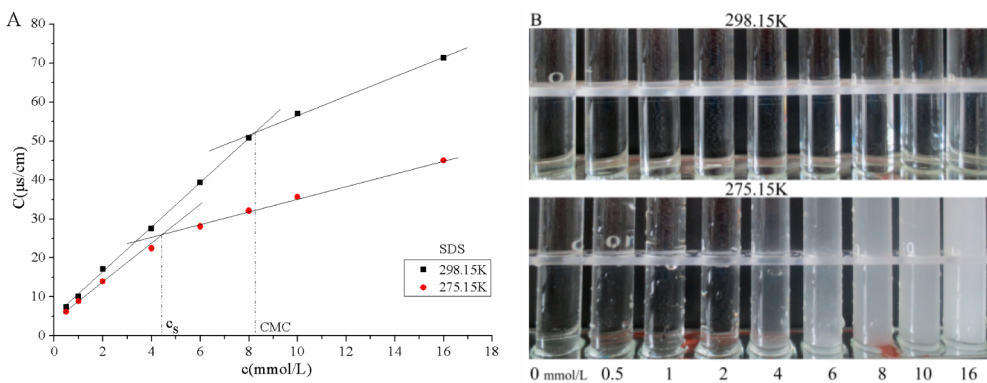


Figure 3. Conductivities (A) and photographs (B) of SDS solutions at 298.15 and 275.15 K (each data point of the conductivities was the average of three measurement values).

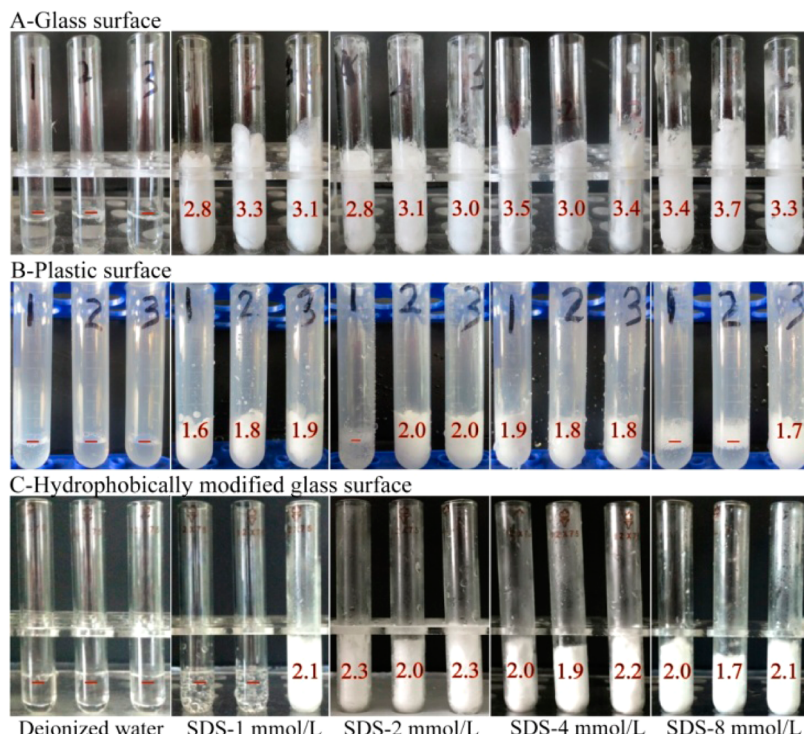


Figure 4. Methane hydrate growth morphology on a glass surface (A), a plastic surface (B), and a hydrophobically modified glass surface (C). (The reaction solution in each tube was 1 mL, the initial pressure was 6 MPa, the temperature was 275.15 K, and the red number was the cover factor.)

Calculation of Methane Consumption. The calculation of methane consumption (n) is shown as follows, and the details of the deviation process were shown in our previous study.¹⁶

$$n = \frac{\frac{P_0 V_0}{z_0 R T_0} - \frac{P_t V_t}{z_t R T_t}}{1 - \frac{P_t \Delta V m}{z_t R T_t}} \quad (3)$$

where P_0 and P_t are the pressures of the reactor at times 0 and t , respectively; T_0 and T_t are the temperatures of the reactor at times 0 and t , respectively; V_0 and V_t are the volumes of the gas phase at times 0 and t , respectively; R is the universal gas constant; m is the theoretical hydration number, which is 5.75 for methane hydrates;¹⁹ ΔV is the molar volume difference between hydrates and water;¹⁸ z_0 and z_t are the compressibility factors at times 0 and t , respectively, which are calculated through the Pitzer correlations for the compressibility factor;²⁰ and the calculation formula is derived as follows:

$$z_t = 1 + \left[0.083 - 0.422 \left(\frac{T_c}{T_t} \right)^{1.6} \right] \frac{P_t T_c}{P_c T_t} + \omega \left[0.139 - 0.172 \left(\frac{T_c}{T_t} \right)^{4.2} \right] \frac{P_t T_c}{P_c T_t} \quad (4)$$

where P_t and T_t are the pressure and temperature of the reactor respectively at time t ; for methane, T_c is 190.6 K; P_c is 4.599 MPa; ω is 0.012.

RESULTS AND DISCUSSION

Critical Micelle Concentration and Solubility of Sodium Dodecyl Sulfate. Figure 3A shows the curves of conductivity vs SDS concentration at room temperature (298.15 K) and hydrate formation temperature (275.15 K). The inflection point of the curve appeared at 8.2 mmol/L at 298.15 K, which might be caused by the formation of micelles. Therefore, the cmc of SDS at 298.15 K ($\text{cmc}^{298.15\text{K}}$) was considered as 8.2 mmol/L in his work, which was reported as 7.8 mmol/L by Di Profio et al.²¹ At 275.15 K, the inflection

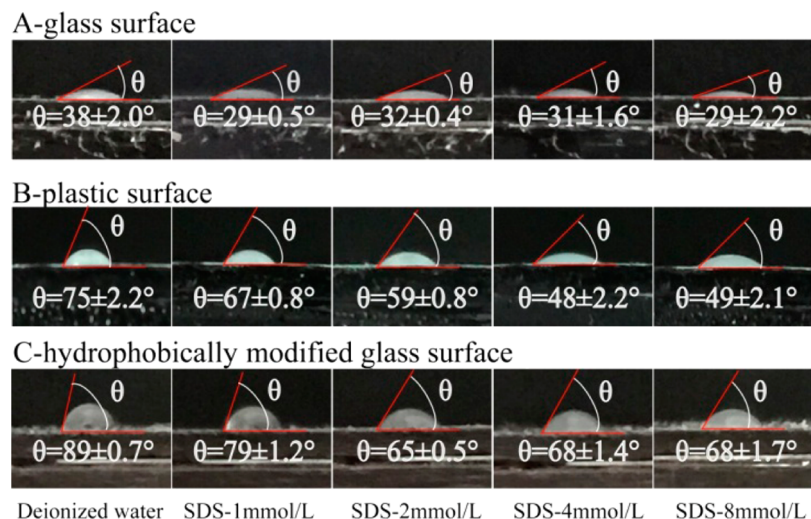


Figure 5. Contact angles of SDS solutions on the surface of glass (A), plastic (B), and hydrophobically modified glass surface (C) at 275.15 K. (The volume of the droplet was 1 μL .)

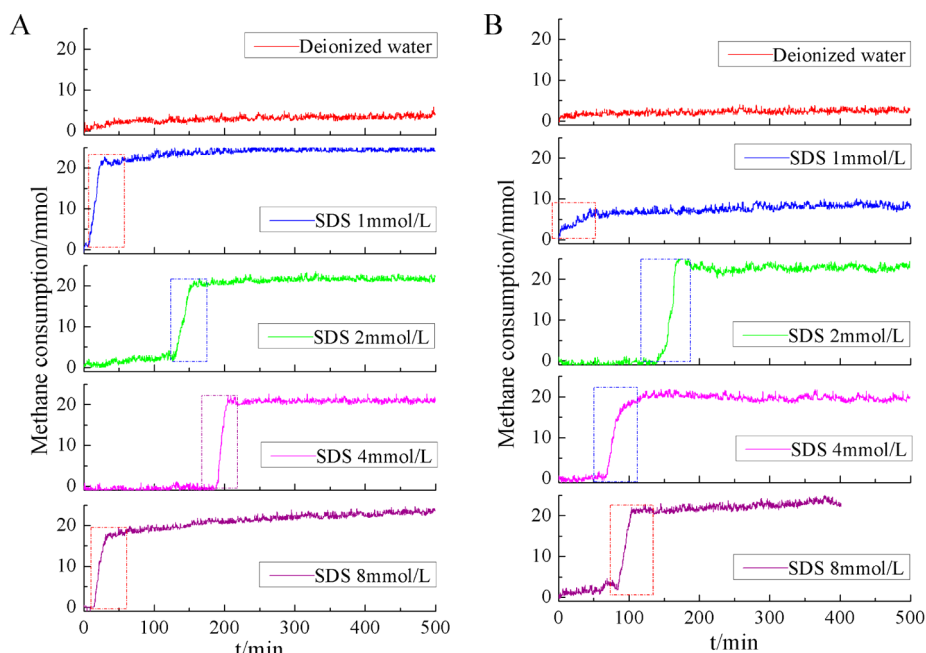


Figure 6. Methane consumption during methane hydrate formation on the glass surface (A) and the hydrophobically modified glass surface (B) (initial pressure, 6 MPa; temperature, 275.15 K).

point of the curve appeared at 4.4 mmol/L. As shown in Figure 3B, SDS precipitated obviously from 6 mmol/L; therefore, the inflection point at 275.15 K might be caused by the precipitation of SDS, and 4.4 mmol/L was considered as the solubility of SDS at 275.15 K (C275.15K S), which was reported as 6.1 mmol/L by Zhang et al.²²

Methane Hydrate Growth on Different Surfaces.

Figure 4A shows the hydrate growth morphology on the glass surface, and all of the hydrate formations with SDS solutions showed obvious upward hydrate growth. Watanabe et al.¹⁰ reported that hydrate formation initially took place with the SDS solution films splashed on the reactor sidewall when charging the reaction solution into the reactor. However, in this work, SDS solution was directly injected into the bottom of the reactor with a pipet, and the splash was avoided. Therefore, hydrate formation might initially take place on the interline of

gas/liquid/solid (reactor sidewall), as reported by Yoslim et al.¹³ As shown in Figure 5A, SDS solutions produced very low contact angles on the glass surface, which indicated a high hydrophilicity of the glass surface and good wettability of the glass surface with SDS solutions. The good wettability was conducive to the up-diffusion of the SDS solution on the glass surface, which caused the upward hydrate growth.¹⁶ Then with the formation of porous hydrate layers on the glass surface, hydrates continued to grow upward under capillary effect. This was consistent with our previous study when SDS was fixed on the surface of polystyrene nanospheres in methane hydrate formation; the contact angle of the SDS solution (1 mmol/L) on the reactor sidewall was increased from $51.9 \pm 1.5^\circ$ to $96.2 \pm 1.1^\circ$, which meant a much poorer wettability; as a result, hydrates no more grew upward on the reactor sidewall but mainly formed in the bottom of the reactor.¹⁵

In addition, Figure 5A also shows that SDS solutions with different concentrations produced similar contact angles, therefore leading to similar cover factors of methane hydrates (Figure 4A), indicating that the upward hydrate growth was mainly affected by the hydrophilicity of the surface, not the SDS concentration. Even the precipitation of SDS (8 mmol/L shown in Figure 3B) did not affect the upward hydrate growth. Therefore, when a plastic surface, with a higher contact angle and poorer hydrophilicity compared to a glass surface (Figure 5A,B), was used, the upward hydrate growth was obviously controlled and much lower cover factors were achieved, as shown in Figure 4B. One possible reason was that glass showed better thermal conductivity than plastic. Another reason might be that the poorer hydrophilicity was less conducive to the up-diffusion of SDS solution on the plastic surface, leading to the less extent of upward hydrate growth. Moreover, Figure 4B and Figure 5B also show that the SDS concentration produced no obvious effect on the upward hydrate growth on the plastic surface.

To confirm the feasibility of controlling methane hydrate growth based on the hydrate growth surface properties, the glass surface was hydrophobically modified with amino silicone oil and then applied in methane hydrate formation. As shown in Figure 5A,C, the modified glass surface showed much bigger contact angle compared to the nonmodified one, denoting the much poorer hydrophilicity of the modified glass surface. As a result, compared with the nonmodified glass surface, the hydrophobically modified one was obviously less conducive to the upward growth of hydrates and resulted in much smaller cover factors (Figure 4C).

In addition, it should be noted that different surfaces led to the hydrates formed in the reactor with different morphologies. With the hydrophilic surface, hydrates grew upward on the reactor sidewall and finally accumulated on the reactor sidewall as circular hydrate layers with the middle part hollow, while, with the hydrophobic surface, hydrates formed mainly in the bottom of the reactor and the hydrates were more compact, as shown in Figure 4.

Methane Hydrate Formation Rate. Figure 6A presents the methane consumption during the methane hydrate formation on the glass surface. In the deionized water system, no obvious methane consumption was observed within 3 days, while in the SDS solution system, the induction time was within several hours and the hydrate growth was completed within 30 min. SDS concentration showed no obvious effect on the induction time and hydrate growth rate, which was consistent with the previous study.¹⁶ However, it should be noted that three tubes were used in each experiment, and all of the hydrate formations with SDS solution in the three nonmodified glass tubes took place nearly at the same time, as shown in Figure 6A. Since the hydrate formations in the three tubes were completely independent, it was proposed that the hydrate formation in one tube might promote the hydrate formation in the other two tubes through temperature or pressure fluctuation caused by hydrate formation.²³

When the glass surface was hydrophobically modified, no obvious effect on the induction time and hydrate growth rate was observed, except that hydrate formation with 1 mmol/L SDS only took place in one tube, which might be due to the stochasticity of hydrate formation, because fresh SDS solutions and new tubes were used in each experiment and the SDS solutions, tubes, and experimental conditions were quite the same. Therefore, it could be proposed that hydrophobic

modification could control the hydrate growth pattern without affecting the hydrate formation kinetics.

Direction Controlled Methane Hydrate Growth. To further achieve direction controlled methane hydrate growth, the existing manner of the reaction solution in the reactor was designed. On one hand, the reaction solution was adsorbed in the sponge placed in the bottom of the glass tube (Figure 7A),

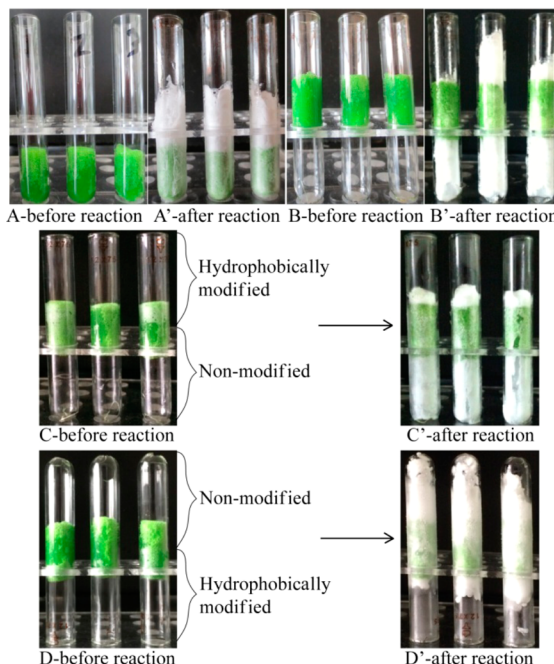


Figure 7. Methane hydrate growth of SDS solution with different existence manners in the reactor (reaction solution, SDS solution, 2 mmol/L; initial pressure, 6 MPa; temperature, 275.15 K).

which meant that the reaction solution was fixed in the bottom of the tube; however, hydrates still grew upward on the glass surface (Figure 7A'). Because the sponge was made of polyurethane, which showed poorer hydrophilicity than the glass surface, SDS solution showed better wettability on the glass surface than that on the sponge. Therefore, although adsorbed in the sponge, the SDS solution could wet the sidewall of the glass reactor and showed up-diffusion on the sidewall during hydrate growth, which resulted in the upward hydrate growth. On the other hand, the reaction solution was fixed in the middle part of the reactor through the sponge (Figure 7B'), at which condition, gravity was used to control the hydrate growth. As a result, although both upward and downward hydrate growth were observed, hydrates grew downward more easily, as shown in Figure 7B'. This was because both capillary effect and gravity affected the hydrate growth direction during the hydrate growth period. When growing upward, the capillary effect had to conquer the gravity, while when growing downward, both the capillary effect and gravity promoted the downward hydrate growth.

In addition, hydrophobic modification was also applied together with the design to the existing manner of the reaction solution in the reactor to control the hydrate growth direction. On one hand, in the hydrate formation with reaction solution fixed in the middle of the reactor, the upper part of the glass surface was hydrophobically modified to hinder the upward hydrate growth (Figure 7C). As a result, almost only downward hydrate growth was observed, as shown in Figure 7C'. On the

other hand, the lower part of the glass surface was hydrophobically modified to retard the downward hydrate growth in the hydrate formation with reaction fixed in the middle of the reactor (Figure 7D). Consequently, although under both capillary effect and gravity, downward hydrate growth was restrained and hydrates mainly grew upward (Figure 7D').

■ CONCLUSIONS

Methane hydrate growth direction was controlled through hydrophobic modification to the hydrate growth surface and design to the existing manner of the reaction solution in the reactor. When a hydrophilic surface (glass) was used in methane hydrate formation, obvious upward hydrate growth was obtained, while when the hydrophobically modified glass surface was applied, the upward hydrate growth was retarded. When the reaction solution was fixed in the middle of the reactor, hydrates mainly grew downward under both gravity and capillary effect. However, when the lower part of the reactor was hydrophobically modified, the downward hydrate growth was restrained and hydrates mainly grew upward.

■ AUTHOR INFORMATION

Corresponding Authors

*(S.-J.L.) E-mail: luosj@qibebt.ac.cn. Fax: 86-532-80662750.
Tel.: 86-532-80662750.

*(R.-B.G.) E-mail: guorb@qibebt.ac.cn. Fax: 86-532-80662708.
Tel.: 86-532-80662708.

Notes

The authors declare no competing financial interest.

■ ACKNOWLEDGMENTS

This work was supported by the National Natural Science Foundation of China (Grants 31101918 and 21307143), the 863 Program (Grant 2011AA060905), Key Projects in the National Science and Technology Pillar Program (Grant 20140015), the Qingdao Science and Technology and People's Livelihood Project (Grant 14-2-3-69 nsh), and the National Key Technology R&D Program (Grants 2013BAD22B00 and 2015BAL04B02).

■ REFERENCES

- (1) Arca, S.; Poletti, L.; Poletti, R.; D'Alessandro, E. *Proceedings of the 7th International Conference on Gas Hydrates (ICGH 2011)*, Jul. 17–21, 2011, Edinburgh, Scotland, United Kingdom; ICGH: Edinburgh, 2011; pp 17–21.
- (2) Pöschl, M.; Ward, S.; Owende, P. *Appl. Energy* **2010**, *87*, 3305–3321.
- (3) Chen, S. Q.; Chen, B. *Appl. Energy* **2014**, *115*, 151–163.
- (4) Sloan, E. D.; Koh, C. A. In *Clathrate Hydrates of Natural Gases*; Heinemann, H., Speight, J. G., Eds.; CRC Press: Boca Raton, FL, USA, 2007; Chapter 1, p 1.
- (5) Zhong, Y.; Rogers, R. E. *Chem. Eng. Sci.* **2000**, *55*, 4175–4187.
- (6) Zhou, L.; Liu, J.; Su, W.; Sun, Y.; Zhou, Y. P. *Energy Fuels* **2010**, *24*, 3789–3795.
- (7) Mori, Y.; Mochizuki, T. *Second International Symposium on Gas Hydrates*, Toulouse, France; ICGH: 1996; pp 267–274.
- (8) Herri, J.; Gruy, F.; Cournil, M. *Second International Symposium on Gas Hydrates*, Toulouse, France; ICGH: 1966; pp 243–250.
- (9) Gayet, P.; Dicharry, C.; Marion, G.; Graciaa, A.; Lachaise, J.; Nesterov, A. *Chem. Eng. Sci.* **2005**, *60*, 5751–5758.
- (10) Watanabe, K.; Imai, S.; Mori, Y. H. *Chem. Eng. Sci.* **2005**, *60*, 4846–4857.
- (11) Okutani, K.; Kuwabara, Y.; Mori, Y. H. *Chem. Eng. Sci.* **2008**, *63*, 183–194.
- (12) Zhang, J. S.; Lee, S.; Lee, J. W. *Ind. Eng. Chem. Res.* **2007**, *46*, 6353–6359.
- (13) Yoslim, J.; Linga, P.; Englezos, P. *J. Cryst. Growth* **2010**, *313*, 68–80.
- (14) Lee, J. D.; Song, M.; Susilo, R.; Englezos, P. *J. Cryst. Growth Des.* **2006**, *6*, 1428–1439.
- (15) Wang, F.; Luo, S. J.; Fu, S. F.; Jia, Z. Z.; Dai, M.; Wang, C. S.; Guo, R. B. *J. Mater. Chem. A* **2015**, *3*, 8316–8323.
- (16) Wang, F.; Jia, Z. Z.; Luo, S. J.; Fu, S. F.; Wang, L.; Shi, X. S.; Wang, C. S.; Guo, R. B. *Chem. Eng. Sci.* **2015**, DOI: [10.1016/j.ces.2015.07.021](https://doi.org/10.1016/j.ces.2015.07.021).
- (17) Anderson, F. E.; Prausnitz, J. M. *AIChE J.* **1986**, *32*, 1321–1333.
- (18) Makogon, Y. F. In *Hydrates of hydrocarbons*; Dunlap, W., Ed.; Pennwell Books: Tulsa, OK, USA, 1997; pp 35–37.
- (19) Gutt, G.; Asmussen, B.; Press, W.; Johnson, M. R.; Handa, Y. P.; Tse, J. S. *J. Chem. Phys.* **2000**, *113*, 4713.
- (20) Smith, J. M.; Van Ness, N. H. C.; Abbott, M. M. In *Introduction to Chemical Engineering Thermodynamics*. McGraw-Hill Education: Singapore, 2001; pp 96–98.
- (21) Di Profio, P.; Arca, S.; Germani, R.; Savelli, G. *Chem. Eng. Sci.* **2005**, *60*, 4141–4145.
- (22) Zhang, J. S.; Lee, S.; Lee, J. W. *J. Colloid Interface Sci.* **2007**, *315*, 313–318.
- (23) Li, X. S.; Xu, C. G.; Chen, Z. Y.; Wu, H. J.; Cai, J. *J. Nat. Gas Chem.* **2011**, *20*, 647–653.